

Comments on the characterisation of oxidation catalysts using TPR/TPO

Nianxue Song^a, Colin Rhodes^a, David W. Johnson^b, and Graham J. Hutchings^{a,*}

^aDepartment of Chemistry, Cardiff University, P.O. Box 912 Cardiff, CF10 3TB UK

^bWilton Centre, Lucite International UK Ltd., Wilton, Redcar, TS10 4RF UK

Received 10 March 2005; accepted 19 April 2005

Temperature programmed reduction (TPR) and oxidation (TPO) are used extensively in catalyst characterisation. In this paper, we examine the use of TPR/TPO cycles for the characterisation of a range of molybdates and single oxides. In particular we observe that the first cycle differs from that of subsequent analyses, even when the maximum temperature is limited to that used in the catalytic reaction. The effect is independent of heating rates and cooling atmospheres and has been demonstrated using different bed configurations. This observation has significance when these oxides are used in periodic flow reactors that involve many cyclical reduction/oxidation.

KEY WORDS: temperature programmed reduction; TPR; temperature programmed oxidation; TPO; TPR/TPO cycles; reduction/oxidation.

1. Introduction

Temperature programmed oxidation (TPO) and temperature programme reduction (TPR) have become essential techniques for catalyst characterisation. Many use TPO and TPR during catalyst preparation to determine optimal calcination and reduction temperatures, respectively. However, it is tempting to use the techniques in more depth, particularly for oxidation catalysts where the catalysts are subjected to reduction/oxidation cycles.

The use of TPR has been widespread since Robertson *et al.* [1] characterised NiO and CuO catalysts and this early work has been reviewed [2]. TPO is an important extension [3] and both techniques depend on great care being taken with the experimental conditions, for example reactant concentration (both gases and catalyst), flowrates, temperature (both ramp rate and final) and reactor dimensions. For example, these effects can lead to significantly different TPR profiles being obtained for Co₃O₄, with two distinct reduction processes [4–6], one distinct with a lower temperature shoulder [7,8] and a single reduction process [9–11]. Monti and Balker [12], fortunately, have made a significant contribution to this difficult topic and they have defined the experimental conditions that are required to achieve reproducible and useable data.

Our attention to this area was prompted by the observation that there is an increased interest in the last 20 years of using periodic or pulse flow reactors, during which time the catalyst is sequentially reduced

and then subsequently reoxidised. During continuous flow oxidation the catalyst is not, typically, subjected to substantial reduction and in such cases TPR/TPO is only valuable in characterising the initial catalyst and *in situ* techniques are required to follow the structural changes occurring during use [13]. However, in periodic flow the oxidation catalyst is substantially reduced and we consider that the use of cyclic TPR/TPO can be of value in characterising oxides for use in periodic flow reactors.

Initial interest in periodic flow reactors for oxidation was prompted by Contractor and co-workers [14–18] who developed the riser/circulating fluidised bed (CFB) reactor for the oxidation of butane to maleic anhydride. In the CFB process, butane is reacted with the vanadium phosphate catalyst in the absence of air in a riser reactor. This permits the catalyst and hydrocarbon to remain in contact for a few seconds at the reaction temperature. Subsequently, the reaction products are recovered and the catalyst is re-oxidised in a fluidised bed by reaction with air. Decoupling the catalyst reduction and re-oxidation stages of the catalyst operation leads to improved process control. Recently Contractor *et al.* [19] have shown the approach can be useful for the ammoxidation of propene and very high selectivity has been reported. Consequently the use of periodic flow reactors is now attracting increased attention for both gas–gas and gas–liquid reaction systems [20–25].

In this paper we examine the use of cyclic TPR/TPO to emulate catalyst reduction and reoxidation during periodic flow for a range of unsupported mixed molybdate and single oxides, and unexpectedly we

*To whom correspondence should be addressed.

E-mail: hutch@cardiff.ac.uk

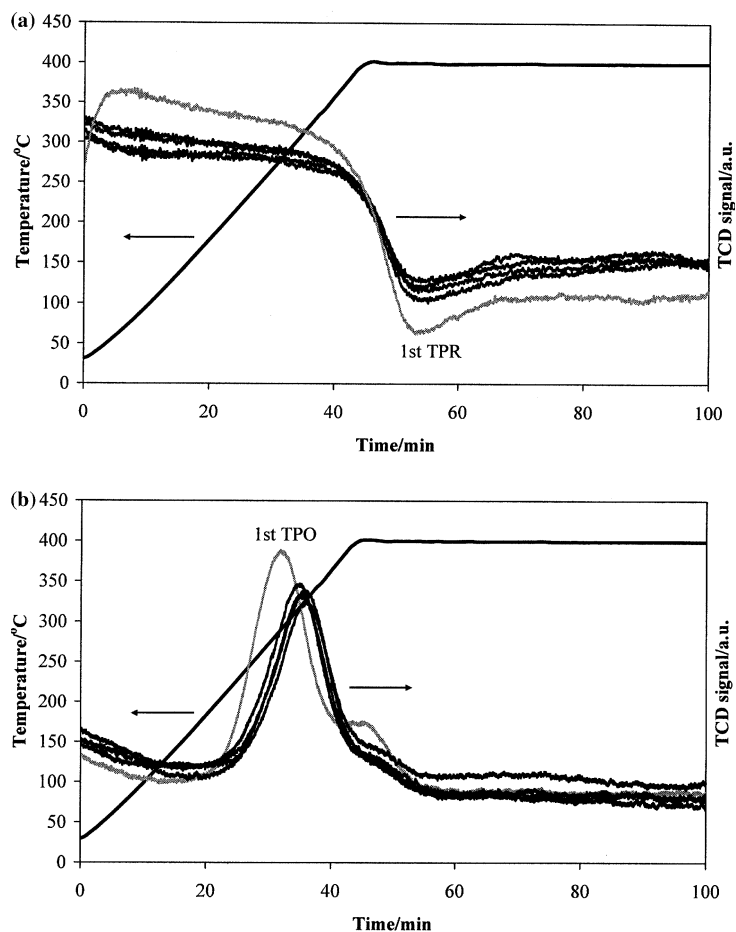


Figure 1. Characterisation of Bi_2MoO_6 using 5 TPR/TPO cycles (TPR first) (a) TPR; (b) TPO. Conditions: $10\text{ }^\circ\text{C min}^{-1}$. TPR: 10% H_2/Ar , 50 ml min^{-1} . TPO: 10% O_2/He , 50 ml min^{-1} . (Grey line denotes 1st TPR or TPO, applied to the whole paper).

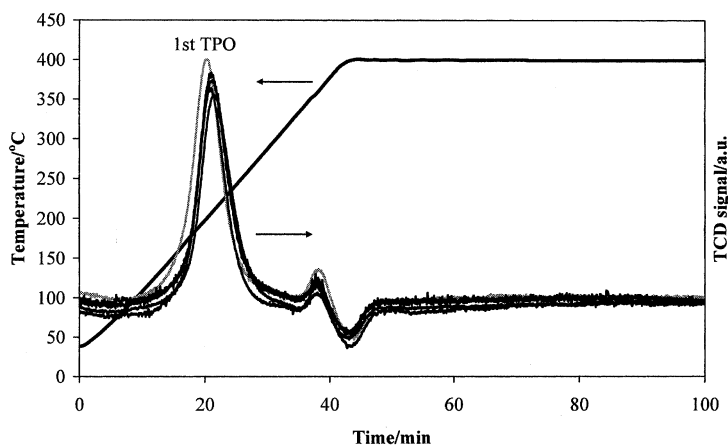


Figure 2. TPO characterisation of Bi_2MoO_6 using 5 TPR/TPO cycles (TPR first). Conditions: $10\text{ }^\circ\text{C min}^{-1}$. TPR: 4% isobutene/He, 50 ml min^{-1} . TPO: 10% O_2/He , 50 ml min^{-1} .

observe that the first temperature programmed cycle gives significantly different results even when the final temperature is the same as that when the catalysts are used in periodic flow reactors.

2. Experimental

Bismuth molybdate binary oxide Bi_2MoO_6 was prepared using a coprecipitation method. $\text{Bi}(\text{NO}_3)_3 \cdot 5\text{H}_2\text{O}$

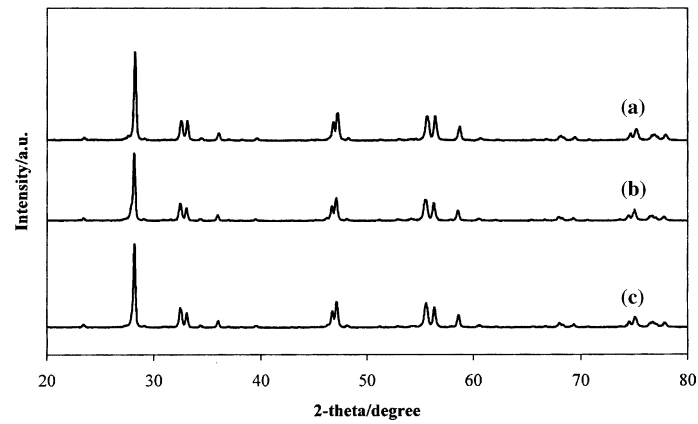


Figure 3. Powder X-ray diffraction patterns for Bi_2MoO_6 catalyst (a) fresh calcined catalyst, (b) after $\text{TPR}_1/\text{TPO}_1$, (c) after $\text{TPR}_1/\text{TPO}_1/\dots/\text{TPR}_5/\text{TPO}_5$.

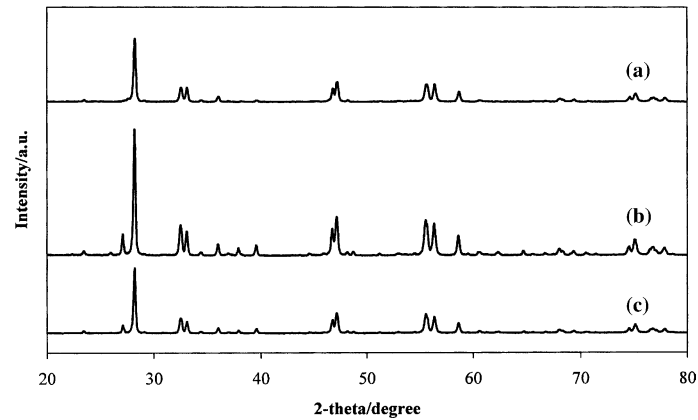


Figure 4. Powder X-ray diffraction patterns for Bi_2MoO_6 catalyst (a) fresh calcined catalyst, (b) after TPR_1 , (c) after $\text{TPR}_1/\text{TPO}_1/\text{TPR}_2$.

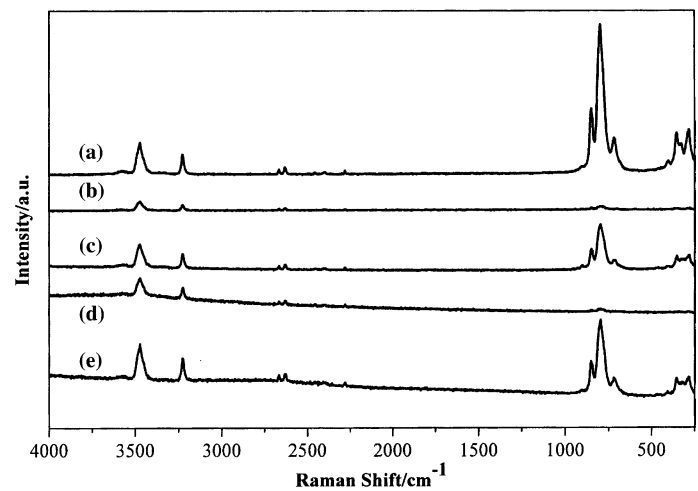


Figure 5. Laser Raman spectra for Bi_2MoO_6 (a) fresh calcined catalyst, (b) after TPR_1 , (c) after $\text{TPR}_1/\text{TPO}_1$, (d) after $\text{TPR}_1/\text{TPO}_1/\text{TPR}_2$, (e) after $\text{TPR}_1/\text{TPO}_1/\dots/\text{TPR}_5/\text{TPO}_5$.

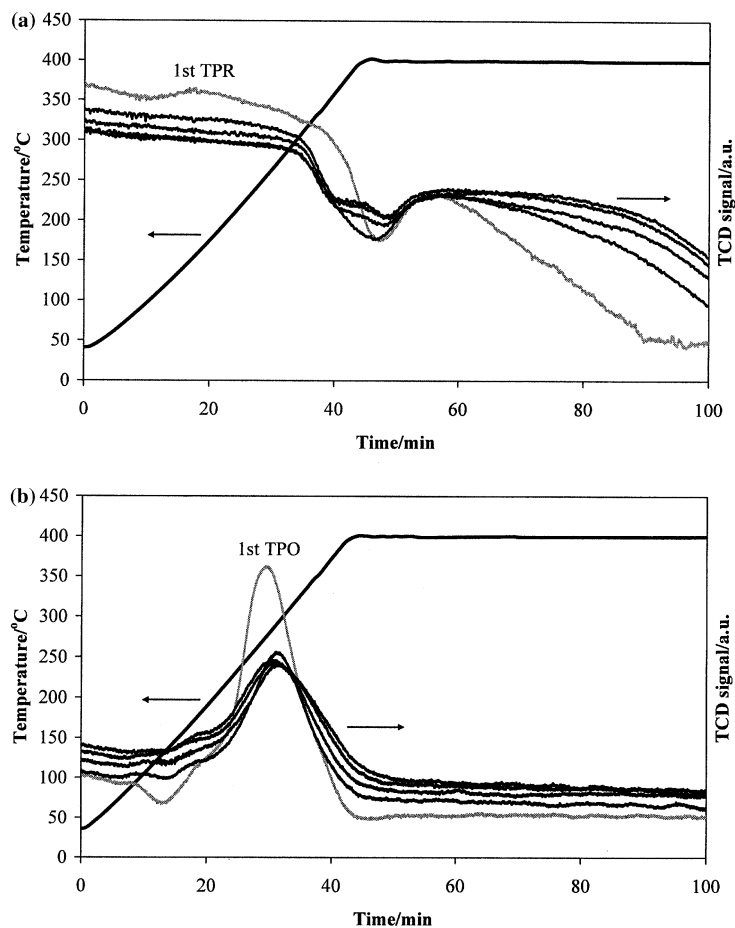


Figure 6. Characterisation of CoMoO_x using 5 TPR/TPO cycles (TPR first) (a) TPR; (b) TPO. Conditions: $10\text{ }^\circ\text{C min}^{-1}$. TPR: 10% H_2/Ar , 50 ml min^{-1} . TPO: 10% O_2/He , 50 ml min^{-1} .

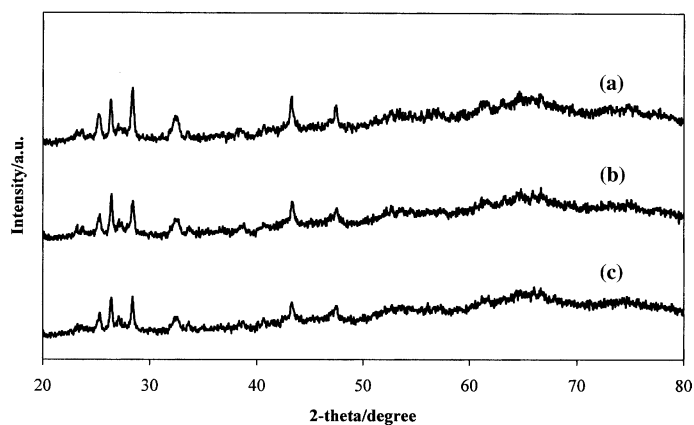


Figure 7. Powder X-ray diffraction patterns for CoMoO_x catalyst (a) fresh calcined catalyst, (b) after TPR₁, (c) after TPR₁/TPO₁/TPR₂.

(25.8 g, Fisher Chemicals) was dissolved in nitric acid (108 ml, 5 M, Fisher Chemicals) at $25\text{ }^\circ\text{C}$ to give solution A. $(\text{NH}_4)_6\text{Mo}_7\text{O}_{24}\cdot 4\text{H}_2\text{O}$ (4.7 g, Fisher Chemicals) was dissolved in aqueous ammonia (108 ml, 5%, Fisher Chemicals) at $25\text{ }^\circ\text{C}$ to give solution B. Solution A was

added dropwise to solution B over 15 min at $25\text{ }^\circ\text{C}$ with stirring. The pH was adjusted to pH 7 with 5% aqueous ammonia. The slurry was heated at $80\text{ }^\circ\text{C}$ for 16 h to give a paste that was dried in air ($100\text{ }^\circ\text{C}$, 24 h) and calcined at $480\text{ }^\circ\text{C}$ for 12 h in air.

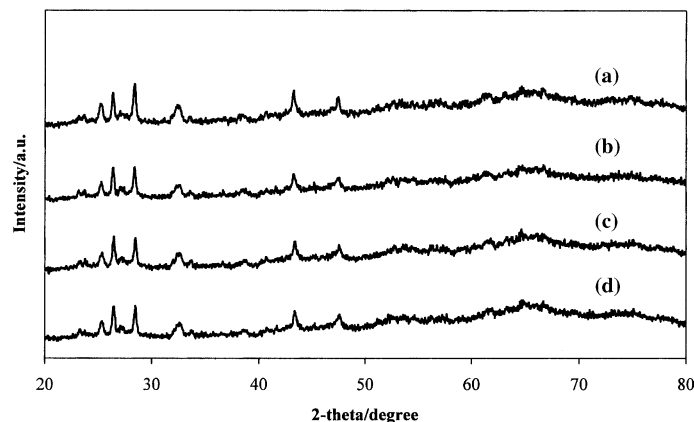


Figure 8. Powder X-ray diffraction patterns for CoMoO_x catalyst (a) fresh calcined catalyst, (b) after $\text{TPR}_1/\text{TPO}_1$, (c) after $\text{TPR}_1/\text{TPO}_1/\text{TPR}_2/\text{TPO}_2$, (d) after $\text{TPR}_1/\text{TPO}_1/\dots/\text{TPR}_5/\text{TPO}_5$.

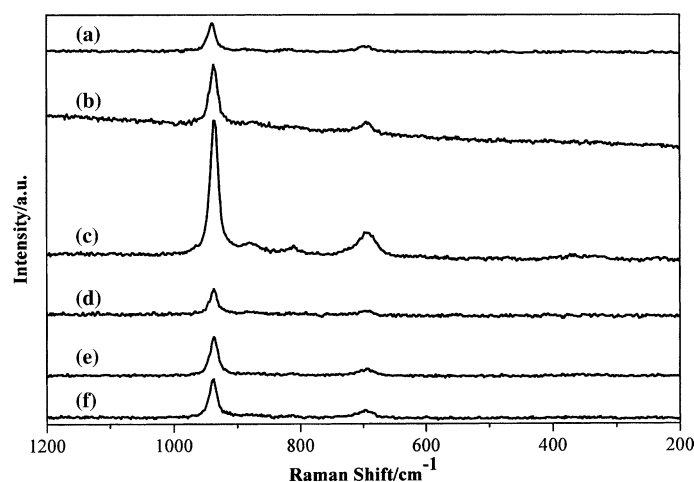


Figure 9. Laser Raman spectra for CoMoO_x (a) fresh calcined catalyst, (b) after TPR_1 , (c) after $\text{TPR}_1/\text{TPO}_1$, (d) after $\text{TPR}_1/\text{TPO}_1/\text{TPR}_2$, (e) after $\text{TPR}_1/\text{TPO}_1/\text{TPR}_2/\text{TPO}_2$, (f) after $\text{TPR}_1/\text{TPO}_1/\dots/\text{TPR}_5/\text{TPO}_5$.

CoBiMoO_x , was prepared as follows. $\text{Bi}(\text{NO}_3)_3 \cdot 5\text{H}_2\text{O}$ (18.3 g, Fisher Chemicals) was dissolved in nitric acid (76 ml, 5 M, Fisher Chemicals) at 25 °C to give solution A. $(\text{NH}_4)_6\text{Mo}_7\text{O}_{24} \cdot 4\text{H}_2\text{O}$ (6.7 g, Fisher Chemicals) was dissolved in aqueous ammonia (120 ml, 5%, Fisher Chemicals) at 25 °C to give solution B. $\text{Co}(\text{NO}_3)_2 \cdot 6\text{H}_2\text{O}$ (10.8 g, Fisher Chemicals) was dissolved in water (140 ml) at 25 °C to give solution C. Solution C was added dropwise to solution A over 5 min at 25 °C. The mixed solution was then added dropwise to solution B over 10 min at 25 °C. The pH was adjusted to pH 7 with 5% aqueous ammonia and the catalyst was recovered and treated as described above.

CoMoO_x was prepared as follows. $\text{Co}(\text{NO}_3)_2 \cdot 6\text{H}_2\text{O}$ (29.1 g, Fisher Chemicals) and $(\text{NH}_4)_6\text{Mo}_7\text{O}_{24} \cdot 4\text{H}_2\text{O}$ (17.6 g, Fisher Chemicals) were dissolved in water (250 ml) at 25 °C. The solution was heated to 80 °C and a blue precipitate formed. The slurry was maintained at this temperature to evaporate most of the water. The resulting paste was dried at 100 °C for 1 h and calcined at 500 °C for 2 h.

A multi-component catalyst, $\text{BiMo}_{12}\text{Fe}_2\text{NiCo}_7\text{MgSb}_{0.9}\text{Ti}_{0.1}\text{Te}_{0.02}\text{Cs}_{0.0}\text{O}_x$, was prepared using the literature method [26]. A number of techniques were used to characterise the materials. Powder X-ray diffraction was performed using an Enraf Nonius FR590 X-ray generator with a Cu-K_α source fitted with an Inel CPS120 hemispherical detector. Raman spectra were obtained using a Renishaw Ramanscope 1000 spectrograph fitted with a green Ar^+ laser ($\lambda = 514.532$ nm). Temperature programmed reduction and temperature programmed oxidation studies were carried out using a Micromeritics AutoChem 2910 instrument using 0.1–0.2 g catalyst.

3. Results and discussion

Our initial experiments were conducted using Bi_2MoO_6 a material that is known to be an active oxidation catalyst [27] and in a separate study we confirmed that our material was active for the oxidation of isobutene with similar activity/selectivity to that

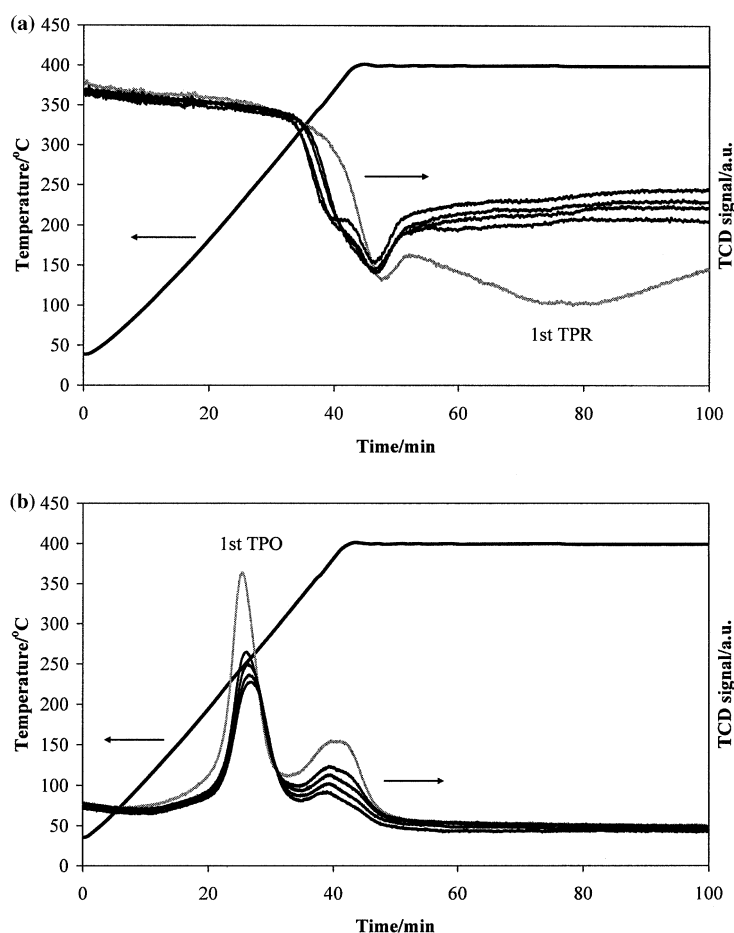


Figure 10. Characterisation of CoBiMoO_x using 5 TPR/TPO cycles (TPR first) (a) TPR; (b) TPO. Conditions: $10\text{ }^\circ\text{C min}^{-1}$. TPR: 10% H_2/Ar , 50 ml min^{-1} . TPO: 10% O_2/He , 50 ml min^{-1} .

reported previously. In our initial studies we have investigated using five cycles of TPO/TPR or TPR/TPO using dilute H_2 (10% H_2 in Ar) or dilute isobutene (4% isobutene in He) as the reducing agents and dilute O_2 (10% O_2 in He) as the oxidant. In these experiments, the temperature was ramped to $400\text{ }^\circ\text{C}$ and held constant at this temperature. We selected this maximum temperature as it is typical of that used in riser reactor/periodic flow reactors for molybdate catalysts, it was also lower than the calcination temperature used to prepare the materials. Typical data for this cyclic TPR/TPO study (i.e. the reduction step is first *cf* simulating use in a riser reactor) are shown in Figure 1 for H_2 as the reducing agent and Figure 2 for isobutene as the reducing agent. The data for the TPR cycles when isobutene is used as reducing agent are complicated since the positive isobutene consumption peak and negative products peaks overlaid each other and this made it impossible to identify the TPR peaks, hence only the TPO data are shown. However, in both cases, the initial TPR and TPO are significantly different from the subsequent TPR/TPO profiles. The effect is also observed identically if the TPO is carried out first. It is also observed if higher

maximum temperatures are used, and we have examined temperatures up to $700\text{ }^\circ\text{C}$. Furthermore, the effect is independent of the atmosphere in which the sample is cooled after the first analysis as we have observed identical data when the catalyst sample is cooled in the reaction atmosphere or in helium or argon. In addition, we have examined the effect of different heating rates to achieve the maximum temperature and again we have observed the same effects when using heating rates of 2, 6, 10 and $18\text{ }^\circ\text{C min}^{-1}$.

To determine that the effect was not an artefact associated with the commercial TPR/TPO apparatus we used, we constructed a TPR/TPO apparatus that allowed us to explore different bed shapes. Again, in all cases the initial TPR/TPO was different from the subsequent experiments. We have conducted many tens of experiments and have observed this effect reproducibly.

Characterisation of the catalysts following H_2 -TPR/TPO cycles using powder X-ray diffraction (Figures 3 and 4) and laser Raman spectroscopy (Figure 5) do not show any significant difference between the first and subsequent oxidation cycles. However, after the reduction step an additional reflection at $d = 0.3289\text{ nm}$ is

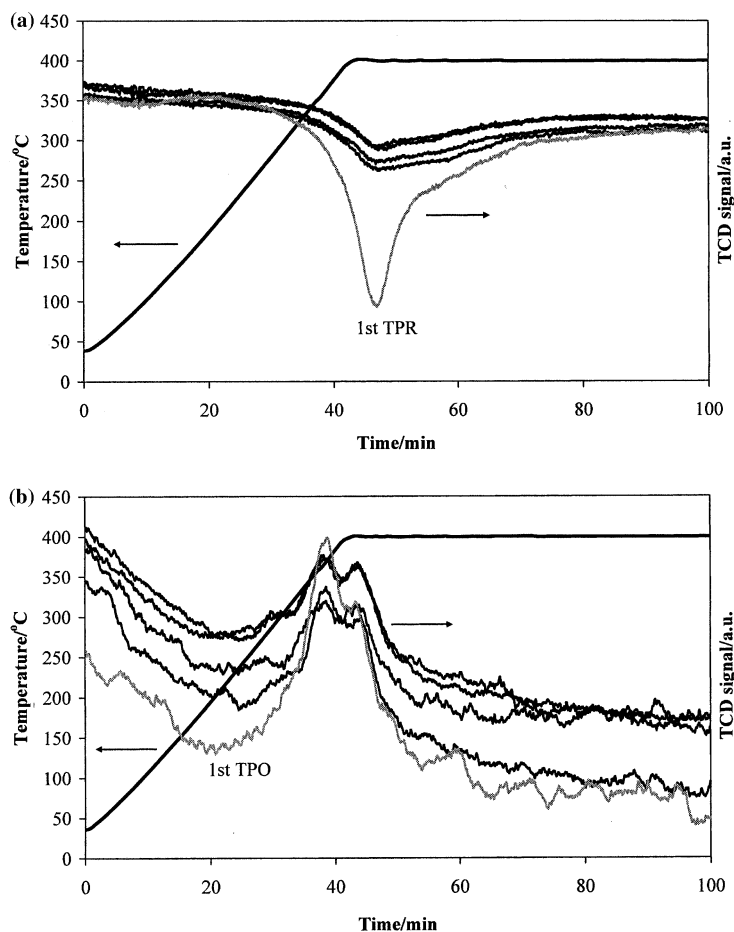


Figure 11. Characterisation of $\text{BiMo}_{12}\text{Fe}_2\text{NiCo}_7\text{MgSb}_{0.9}\text{Ti}_{0.1}\text{Te}_{0.2}\text{Cs}_{0.4}\text{O}_x$ using 5 TPR/TPO cycles (TPR first) (a) TPR; (b) TPO. Conditions: $10^\circ\text{C min}^{-1}$. TPR: 10% H_2/Ar , 50 ml min^{-1} . TPO: 10% O_2/He , 50 ml min^{-1} .

observed. This reflection is considered to be the (0 1 2) plane of metallic bismuth ($d = 0.328\text{ nm}$). It is clear that the reduction step is causing a bulk structural change, although this is not particularly apparent in the Raman spectra. It is possible therefore that the effects we observe between the first and subsequent TPR/TPO cycles could be due to this structural change. Hence we have investigated a range of further catalytic materials. The data for CoMoO_x are shown in Figure 6. Again the first TPR/TPO is different from the subsequent cycles. In this case the structural investigation using X-ray powder diffraction (Figures 7 and 8) and Raman spectroscopy (Figure 9) show there are no structural differences induced by the TPR experiments and consequently we do not consider the difference observed with the first cycle for Bi_2MoO_6 is related to structural changes.

Subsequently, we examined a mixed cobalt bismuth molybdate CoBiMoO_x and a complex molybdate catalyst $\text{BiMo}_{12}\text{Fe}_2\text{NiCo}_7\text{MgSb}_{0.9}\text{Ti}_{0.1}\text{Te}_{0.02}\text{Cs}_{0.4}\text{O}_x$ that has been reported [26] as an exceptionally active catalyst for isobutene oxidation to methacrolein, and in a separate study we confirmed that both were active and selective for this reaction. Cyclic TPR/TPO data are

shown in Figures 10 and 11, respectively. Again the first TPR/TPO cycle is significantly different from the subsequent cycles.

In view of these findings we examined the TPR/TPO cycles for the major components of the mixed oxides, i.e. MoO_3 , Bi_2O_3 and Co_3O_4 using a maximum temperature of 400°C . With MoO_3 no reduction or oxidation was observed in this temperature range. With Bi_2O_3 the first and subsequent TPR/TPO cycles were, in this case, identical (Figure 12). With Co_3O_4 (Figure 13) the first and subsequent cycles are different as observed with the more complex molybdates. We have also observed this effect with other oxides and it appears that Bi_2O_3 is an exception with respect to its behaviour.

Our results show that for complex molybdates, as well as less complex materials, the first and subsequent TPR/TPO cycles are clearly different. The first cycle being unique. This has consequences for the use of these materials in periodic flow or riser reactors in that the materials will clearly change following the first reduction/oxidation cycle. The effect is almost certainly related to surface oxygen availability and detailed surface studies are now required to examine the origin of this

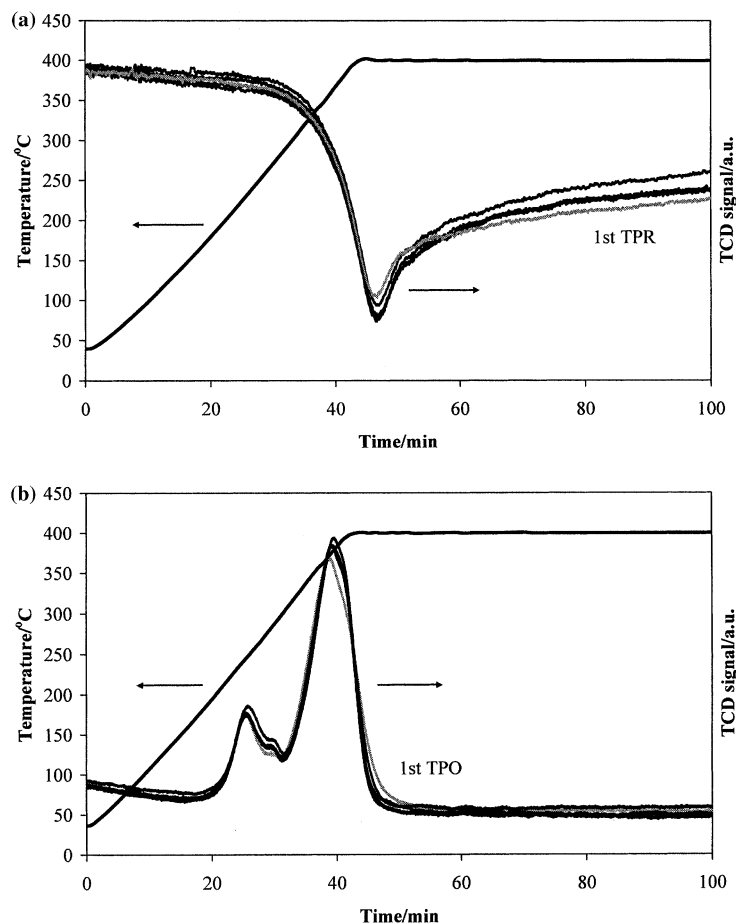


Figure 12. Characterisation of Bi_2O_3 using 5 TPR/TPO cycles (TPR first) (a) TPR; (b) TPO. Conditions: $10\text{ }^\circ\text{C min}^{-1}$. TPR: 10% H_2/Ar , 50 ml min^{-1} . TPO 10% O_2/He , 50 ml min^{-1} .

effect in more detail. However, we have clearly shown that the use of TPR/TPO or TPO/TPR cycles is significantly more informative than single experiments and we advocate this methodology for the study of heterogeneous catalysts in general.

Acknowledgements

We thank ICI Acrylics, Ineos Acrylics and Lucite International for financial support and we thank the Committee of Vice-Chancellors and Principals of the University of the UK for an Overseas Research Student (ORS) award for NS.

References

- [1] S.D. Robertson, B.D. McNicol, J.H. De Baas, S.C. Kloet and J.W. Jenkins, *J. Catal.* 37 (1975) 424.
- [2] N.W. Hurst, S.J. Gentry, A. Jones and B.D. McNicol, *Catal. Rev. Sci. Eng.* 24 (1982) 233.
- [3] B. Jouguet, A. Gervasini and A. Auroux, *Chem. Eng. Technol.* 18 (1995) 243.
- [4] T. Paryjczak, J. Rynkowski and S. Karski, *J. Chromatogr.* 188 (1980) 254.
- [5] B.A. Sexton, A.E. Hughes and T.W. Turney, *J. Catal.* 97 (1986) 390.
- [6] E. van Steen, G.S. Sewell, R.A. Makhothe, C. Micklethwaite, H. Manstein, M. Lange and C.T. O'Connor, *J. Catal.* 162 (1996) 220.
- [7] H.F.J. van't Blik and R. Prins, *J. Catal.* 97 (1986) 188.
- [8] B. Viswanathan and R. Gopalakrishnan, *J. Catal.* 99 (1986) 342.
- [9] M.P. Rosynek and C.A. Polansky, *Appl. Catal.* 73 (1991) 97.
- [10] I. Puskas, T.H. Fleisch, J.B. Hall, B.L. Meyers and R.T. Rogiński, *J. Catal.* 134 (1992) 615.
- [11] H. Ming and B.G. Baker, *Appl. Catal.* 123 (1995) 23.
- [12] D.A.M. Monti and A. Baiker, *J. Catal.* 83 (1983) 323.
- [13] M. Hunger and J. Weitkamp, *Angew. Chem. Int. Ed.* 40 (2001) 2954.
- [14] R.M. Contractor, US Patent 4 668 802 (1987), to E. I. Du Pont de Nemours and Co.
- [15] R.M. Contractor, H.E. Bergna, H.S. Horowitz, C.M. Blackstone, B. Malone, C.C. Torardi, B. Griffiths, U. Chowdhry and A.W. Sleight, *Catal. Today* 1 (1987) 49.
- [16] R.M. Contractor and A.W. Sleight, *Catal. Today* 3 (1988) 175.
- [17] R.M. Contractor, D.I. Garnett, H.S. Horowitz, H.E. Bergna, G.S. Patience, J.T. Schwartz and G.M. Sisler, *Stud. Surf. Sci. Catal.* 82 (1994) 233.
- [18] R.M. Contractor, *Chem. Eng. Sci.* 54 (1999) 5627.
- [19] R.M. Contractor, M.W. Andersen, D. Campos, G. Hecquet, R. Kotwica, C. Pham, M. Simon and M. Stojanovic, US Patent 4 437 193 (2002), to E.I. Du Pont de Nemours and Co.

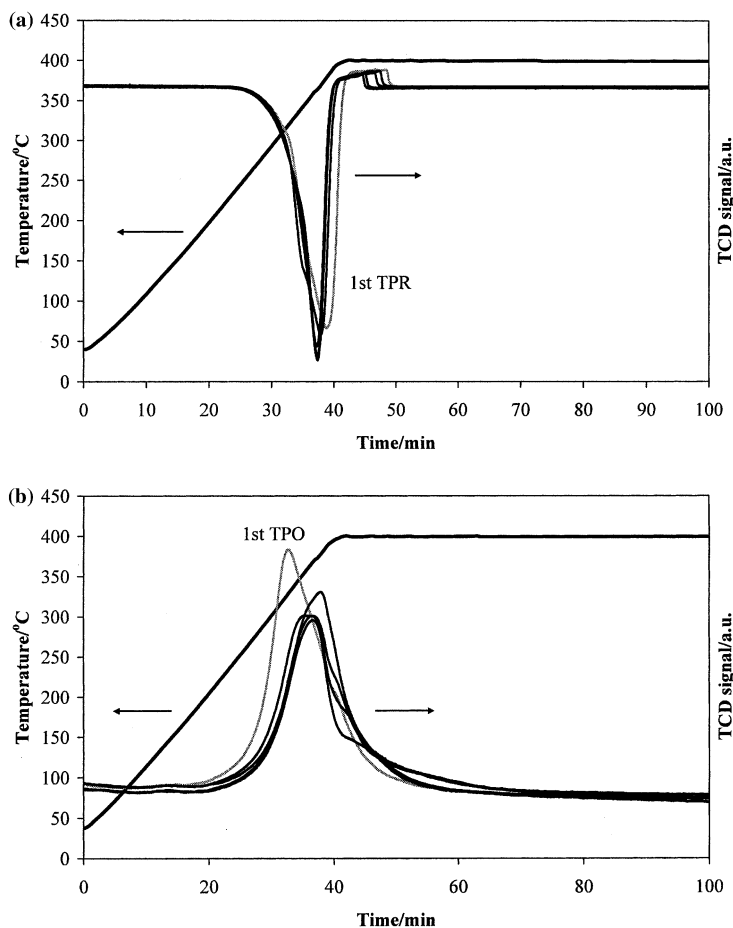


Figure 13. Characterisation of Co_3O_4 using 5 TPR/TPO cycles (TPR first) (a) TPR; (b) TPO. Conditions: $10\text{ }^\circ\text{C min}^{-1}$. TPR: $10\% \text{ H}_2/\text{Ar}$, 50 ml min^{-1} . TPO: $10\% \text{ O}_2/\text{He}$, 50 ml min^{-1} .

- [20] E. Vaitis, D. Chadwick and E. Alpay, Chem. Eng. Res. Des. 82 (2004) 653.
- [21] I. Yongsunthon and E. Alpay, Chem. Eng. Sci. 54 (1999) 2647.
- [22] R. Del Rosso, A. Kaddouri, C. Mazzocchia, P. Gronchi and P. Centola, Catal. Lett. 69 (2000) 71.
- [23] R. Del Rosso, A. Kaddouri, D. Fumagalli, C. Mazzocchia, P. Gronchi and P. Centola, React. Kinet. Catal. Lett. 68 (1999) 175.
- [24] A. Kaddouri, R. Del Rosso, C. Mazzocchia, P. Gronchi and P. Centola, Catal. Lett. 63 (1999) 65.
- [25] R. Del Rosso, A. Kaddouri, D. Fumagalli, C. Mazzocchia, P. Gronchi and P. Centola, Catal. Lett. 55 (1998) 93.
- [26] S. Watanabe, H. Yoshioka and J. Izulni, US Patent 5 856 259 (1999), to Mitsubishi Rayon Co. Ltd.
- [27] D. Carson, G. Coudurier, M. Forissier, J.C. Vedrine, A. Laarif and F. Theobald, J. Chem. Soc., Faraday Trans. 179 (1983) 1921.